AGU PUBLICATIONS

JGR

Journal of Geophysical Research: Biogeosciences

RESEARCH ARTICLE

10.1002/2015JG003288

Special Section:
Carbon and Nitrogen Fluxes at the Land-Ocean Interface

Key Points:
- Substantial sediment organic carbon (OC) trapped in floodplain
- Deposited sediment OC poor, postdeposition OC enrichment occurs
- High mineralization rates and postdepositional loss limiting long-term sink

Supporting Information:
- Supporting Information S1

Correspondence to:
F. O. Omengo,
fredochieng.omengo@kuleuven.be

Citation:
Omengo, F. O., N. Geeraert, S. Bouillon, and G. Govers (2016), Deposition and fate of organic carbon in floodplains along a tropical semiarid lowland river (Tana River, Kenya), *J. Geophys. Res. Biogeosci.*, *121*, doi:10.1002/2015JG003288.

Received 26 NOV 2015
Accepted 28 MAR 2016
Accepted article online 1 APR 2016

Deposition and fate of organic carbon in floodplains along a tropical semiarid lowland river (Tana River, Kenya)

Fred O. Omengo[1,2], Naomi Geeraert[1], Steven Bouillon[1], and Gerard Govers[1]

[1]Department of Earth and Environmental Sciences, Katholieke Universiteit Leuven, Leuven, Belgium, [2]Kenya Wildlife Service, Nairobi, Kenya

Abstract Inland waters organic carbon (OC) burial by sedimentation has recently been shown to be an important component in river catchment carbon (C) budgets. However, data on OC burial by sedimentation are hitherto largely limited to temperate zones. We investigated the deposition and fate of sediment-associated OC in the floodplains of the tropical lowland Tana River (Kenya), between two main gaging stations (Garissa and Garsen). Freshly deposited surface sediments and sediment cores were sampled and analyzed for OC, total nitrogen content, stable isotope signatures ($\delta^{13}C$) of OC, and grain size distribution. In addition, we incubated sediment cores to quantify CO_2 production as a proxy for OC mineralization. While the floodplain receives sediment with a relatively low OC content ($1.56 \pm 0.42\%$), sediments are enriched with OC inputs from floodplain vegetation to levels above 3%. Sediment cores show a sharp decrease of OC with depth, from 3 to 12% OC in the (sub) surface to less than 1% OC below approximately 60 cm depth. Relatively elevated OC mineralization rates (0.14 ± 0.07 mol. CO_2 kgC^{-1} d^{-1}) were recorded. We used these data to make a first assessment of the C burial efficiency of the Tana River floodplain. In contrast to what is observed in temperate environments, over 50% of C present in the top layers is lost in less than a century. While significant amounts of OC are buried in the Tana River floodplain, the high rates of postdepositional loss limit the development of a long-term C sink within this tropical floodplain.

1. Introduction

Rivers are the main link between the terrestrial and oceanic realm; they do not only globally export circa 20 Gt yr^{-1} of sediments but also circa 1 Gt carbon (C) yr^{-1} from the land to the oceans [*Schlünz and Schneider*, 2000; *Lal*, 2003; *Cole et al.*, 2007]. However, rivers do not only transport C, a significant fraction of the total C that enters the rivers from land is outgassed [*Borges et al.*, 2015; *Hotchkiss et al.*, 2015]. Another significant loss term in the fluvial network is the deposition of sediments containing organic carbon (OC) in floodplain environments [*Hunsinger et al.*, 2010]. Within-river photosynthesis, on the other hand, may lead to the "production" of additional OC.

Floodplains are recognized as important sites of sediment and C storage within fluvial networks [e.g., *Hoffman et al.*, 2009] and fluvial geomorphologists recognize that there can be a long (millennial) delay between upland erosion of bulk materials and the discharge of those materials from large river basins to the ocean due to floodplain buffering [e.g., *Meade*, 1996; *Dearing and Jones*, 2003]. The OC that is deposited with sediments may therefore be stored for several centuries, if not millennia in floodplain environments. Studies in the colluvial and alluvial stores in temperate environments suggest that OC may indeed be preserved over considerable periods but that a large fraction of the buried OC will eventually be mineralized [*Galy et al.*, 2007; *Rommens et al.*, 2006; *Van Oost et al.*, 2012]. This mineralization process may take a long time. In loess environments in Belgium, for example, ~50% of the OC that is buried is lost over a period of circa 350 year [*Van Oost et al.*, 2012; *Wang et al.*, 2015].

The studies above have tried to quantify the role of depositional environment as sinks of OC in temperate environments, but information on tropical environments is still limited. Tropical environments differ fundamentally from their temperate counterparts, as they experience higher average temperatures and distinct dry and wet seasons. This may cause these depositional environments to be subjected to much more intense wetting and drying cycles than is the case in temperate environments. These differences may have fundamental effects on the OC mineralization-preservation balance in buried sediments. For example, while higher temperatures will generally lead to increased turnover rates, the alternation of wet and dry states may limit it, given that moisture is a prerequisite for efficient OC mineralization.

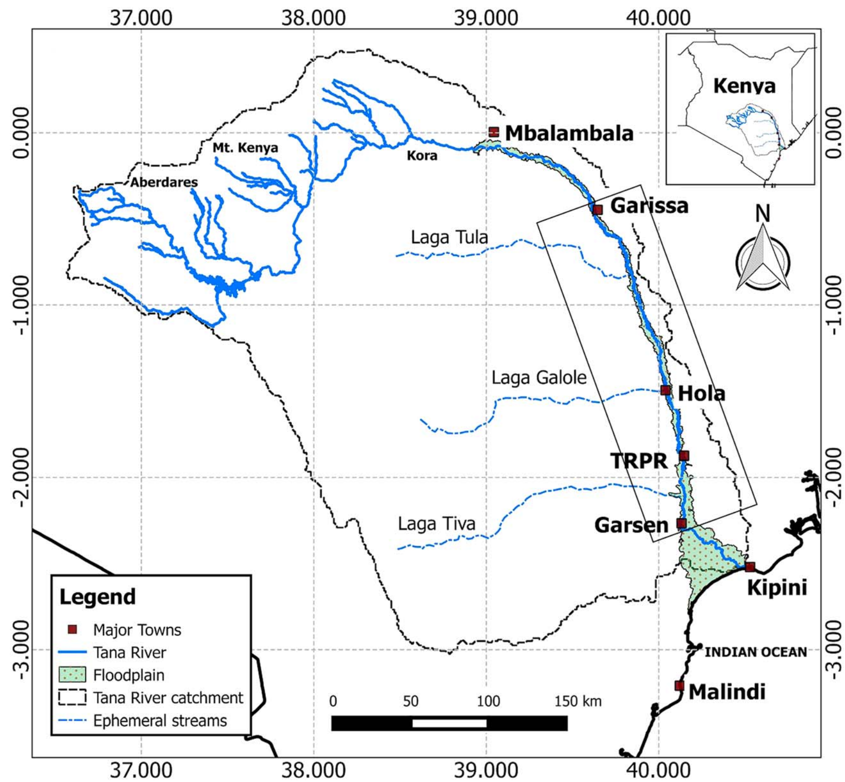

Figure 1. Study area showing the location of the Tana River, Kenya, and the Garissa-Garsen section of the Tana River floodplains. Three ephemeral streams (lagas) join the main river within this reach. Downstream of Garsen there is a shorter but more expansive lower section (Tana River Delta) before the river flows into the Indian Ocean at Kipini. The box between Garissa-Garsen shows the location of the study area where sampling was done.

In order to garner an accurate global assessment of the role of floodplain in C burial, it is important to have information on tropical environments. Here we present a study on C deposition and burial in the Tana River, a tropical river system located in Kenya. The lower Tana River has extensive floodplains and it has been suggested that substantial quantities of sediments and OC are retained within the system [*Tamooh et al*., 2014].

The main objective of the study was to quantify deposition rates and post sedimentation dynamics of OC within the floodplains of Tana River. We focus on a floodplain reach between two gauging stations (Garissa and Garsen), which has very limited inflow from tributaries and at the same time experiences semiannual flooding and sediment deposition cycles. We explore the delivery of fluvial transported sediment and OC to the floodplain, postdepositional processes, changes in OC concentrations, and the role of the Tana floodplain as a long-term OC sink.

2. Materials and Methods

2.1. Study Area

The Tana is the largest river in Kenya with a length of ~1000 km. The river originates in the central highlands surrounding Mount Kenya and the Aberdare mountains, (~5800 m above sea level), with the lower Tana consisting of the section downstream of Kora where the river traverses the landscape for ~700 km through semiarid plains and finally drains into the Indian Ocean (Figure 1). The upper Tana catchment has five hydroelectric dams with a combined reservoir surface area of 150 km^2 [*Brown and Schneider*, 1996; *Maingi and Marsh*, 2002]. The lower Tana has intermittent tributaries (*lagas*, see Figure 1) draining large catchments but which only flow in short pulses during the wet season [*Maingi and Marsh*, 2002].

2.1.1. Climate and Geology

The average annual precipitation varies from ~2200 mm yr^{-1} in the upper Tana catchment to ~370 mm yr^{-1} for the lower Tana between Kora and Garissa. Further downstream, a gradual increase is observed from ~350 mm yr^{-1} at Garissa to ~470 mm yr^{-1} at Hola and over 1000 mm yr^{-1} at areas downstream of Garsen

[*Brown and Schneider*, 1996]. Temperatures are on average above 30°C in the region of the lower Tana, with a mean annual potential evapotranspiration between 1500 and 1700 mm [*Dagg et al.*, 1970].

The geology of the upper Tana catchment has been described as a Precambrian basement complex, with volcanic formations mainly of Tertiary age that originate from Mount Kenya and the Aberdares. These volcanic rocks cover almost two thirds of the upper catchment. Downstream of Kora, the Tana is considered to be an alluvial river and not constricted by outcrops of bedrock; therefore, most of the meandering is determined by morphological processes [*Dwars, Heederik en Verhey*, 1986].

2.1.2. Floodplains

The minimal elevation drop downstream of Mbalambala has resulted in the formation of an extensive floodplain wherein the river is freely meandering. Overbank flows are common and usually associated with increased rainfall in the upper catchment but releases of water from the dams may also contribute. The majority of the floodplains exists either as fallow forest patches for conservation purposes or agricultural hotspots utilized for small scale farming. In areas where the vegetation has been cleared to pave the way for seasonal agriculture, flood waters are used for irrigation and cultivation that is limited to post flooding periods. Occasionally, biomass from agricultural crops is left in the fields but mostly used for livestock feeding.

Throughout the remainder of the floodplain, a characteristic riparian forest fringes the banks of Tana River which consists of a mosaic of deciduous and evergreen trees rich in endemic species [*Medley*, 1992; *Hughes*, 1988]. The forest width varies and in certain areas may reach up to 3 km, while elsewhere it is restricted to only a few meters from the river bank. The riverine forest extends over a length of 400 km along the Tana River from Mbalambala to Kipini and is dependent on flooding and ground water recharge. Within the floodplain forest, seasonal litter, and root biomass input contribute significantly to the soil OC pool.

2.1.3. Hydrology and Flooding

Two annual precipitation cycles occur in the basin, resulting in a bimodal discharge peak and potential flooding. The first annual peak discharge typically occurs between April and June (long rainy season) and a shorter high flow period occurs during November/December (short rainy season). At Garissa, wet season flows generally range between 300 and 700 $m^3 s^{-1}$ while base flow is at a mean of 75 $m^3 s^{-1}$. Occasionally extreme flood events with discharges over 1000 $m^3 s^{-1}$ have been observed, (Water Resources Management Authority, WRMA-KENYA). During high flows, overbank flows are common leading to flooding and waterlogging of floodplain areas. The floods can last more than a month, after which they recede and the floodplains gradually dry up. The water table level in the depositional areas varies based on the location of the area relative to the main river and the time since the last flood event.

2.2. Methods

2.2.1. Field Work

Fieldwork was conducted in October–November 2012, May–July 2013, and February–April 2015. In total, 30 sediment cores were collected during the three campaigns. During the first and third campaigns no substantial flooding occurred, while in the second campaign extensive flooding lasting at least 1 month in most sections of the study area was experienced. During this campaign coring was performed immediately after the recession of flood waters.

During each campaign, coring locations were chosen so that the diversity of depositional environments within the floodplain was covered. During the first and second campaigns, coring was performed with an Eijkelkamp sediment core sampler (Model 04.16, Ø40 × 200 mm), extendable to 2.2 m depth. Sediments were later pushed from the tubes with an Eijkelkamp hand pusher and sliced at 1 cm intervals, air dried, and stored in zipped airtight polyethylene bags. The third campaign involved limited coring at a section of previously sampled areas and involved collection of eight additional cores from selected sites as well as sediment incubation experiments. The incubations were aimed at quantifying CO_2 production and were performed in situ as well as under controlled lab conditions upon return to the home laboratory. For the field incubations, a soil Edelman auger corer was used to extract sediment cores at a predetermined depth and samples were weighed in the field (KERN-KB1200-2 N, accuracy ±0.01 g). Based on the prior estimated OC content, between 20 and 100 g were immediately transferred into 300 mL incubation jars equipped with gas sampling valves. The headspace in the jars was closed immediately and flushed with soda lime to remove excess CO_2 background. Each sample was measured for 7 days with daily incubation of ~8 h and sampling of headspace gas. Field incubation temperatures could not be standardized, but the area was relatively warm with daily temperatures between 28 and 35°C during the time of sampling. For each coring site, an additional core was extracted using a soil auger and samples for bulk density taken at approximately 10 cm depth intervals using a Kopecky ring.

In addition to coring, we undertook postevent surveys [*Gomez et al*., 1995; *Walling et al*., 1997] during the second campaign and collected freshly deposited sediment from various sections of the floodplain ($n = 30$) to establish the quantity of OC in new deposits. Sampling for fresh sediment involved scraping using a small spade and measuring their thickness of the fresh deposition as well as using a tape measure to establish the associated flood height based on surrounding vegetation. The sediments were air dried and stored in zipped plastic bags for later analysis in the lab. Particulate OC (POC) concentrations are based on daily grab samples collected from the middle of the river during the long rainy seasons (20 March 2013 to 21 June 2013, Garissa $n = 49$, Garsen $n = 52$) and are also reported in *Geeraert et al*. [2015a]; 25–100 mL of water was filtered on precombusted (4 h at 450°C) 25 mm Whatman GF/F filters (pore size: 0.7 μm). The filters were air dried in the field and oven dried at 60°C in the lab prior to determining OC concentrations.

2.2.2. Laboratory Analyses

Upon return to the laboratory, bulk density samples were weighed to establish the wet weight and then oven dried at 105°C for 24 h after which they were reweighed to establish the dry weight. The rest of the samples were oven dried at 105°C for 24 h and then ground with a pestle. Particle size distribution was determined using a laser diffraction particle size analyzer (LS13320, Range: 0.02–2000 μm).

To quantify OC content, a weighed subsample was transferred into an Ag cup to which 20–100 μL 10% HCl solution was added to remove all carbonates. Samples were then oven dried at 60°C for 24 h. This procedure was repeated until there was no reaction with HCl. OC, total nitrogen (TN), and the $\delta^{13}C$ of OC were determined with an elemental analyzer—isotope ratio mass spectrometer (Thermo Flash HT/EA and Delta V Advantage) using the thermal conductivity detector (TCD) signal of the EA to quantify TN, and by monitoring m/z 44, 45, and 46 on the isotope ratio mass spectrometer. Acetanilide and IAEA-C6 were used to calibrate the $\delta^{13}C$ and concentration data. Reproducibility of $\delta^{13}C$ measurements was better than ±0.2‰, while relative standard deviations of the calibration standards for OC and TN measurements were typically <2% and always <5% OC:TN ratios are presented on a mass:mass basis.

For the analysis of $\Delta^{14}C$, we selected 12 samples at various depths from one sediment core (Kiluluni III, E1.835 S40.119). Subsamples were acidified with 5% HCl to remove carbonates, combusted in an elemental analyzer, and the resulting CO_2 was cryogenically trapped and purified on a vacuum line. Graphitization of CO_2 and ^{14}C measurements were performed at the Royal Institute for Cultural Heritage (Brussels, Belgium) using a MICADAS (Mini carbon dating system). Measurement of ^{14}C activity are expressed as percentage modern C (pmC) employing a $\delta^{13}C$ correction for isotope fractionation. The ^{14}C content was converted into age (years B.P.) with A.D. 1950 being considered 100 pmC and 0 year B.P.

Sedimentation rates were based on *Omengo et al*. [2016] where radionuclides and a postflood survey of fresh flood deposits was used to quantify floodplain sedimentation rates. An average 50 year mean sedimentation rate of 1.21 ± 0.35 g cm^{-2} yr^{-1} based on ^{137}Cs inventories and a 100 year mean of 1.01 ± 0.50 g cm^{-2} yr^{-1} based on $^{210}Pb_{xs}$ was obtained for the coring sites. Fresh sediment deposits after the 2013 floods averaged of 0.58 ± 0.42 g cm^{-2}, suggesting that average long-term rates were somewhat higher than the deposition rates observed in 2013 or that the sample sites may have, on average, higher sedimentation rates than the floodplain as a whole.

2.2.3. Mineralization Rates

To determine organic matter (OM) mineralization rates, sediment samples were incubated (i) at field conditions (temperatures were between 28–35°C and without sample normalization for moisture) for 7 days and (ii) in the laboratory at ~60% water holding capacity (WHC) and 30°C for 15 days. For the lab incubations, air-dried samples were placed in air-tight jars and gradually wetted to ~60% WHC by slowly adding deionized water. In both setups, the lid of the incubation jars was fitted with three-way valves. At the start of each incubation time interval, the jar was flushed for 2 min with air at ambient CO_2 concentration by allowing the air in through one valve and evacuating through the other valve. After this, the jar was closed and stored in an incubation chamber at the specified temperature for a time period of ~8 h. After each incubation time interval, the headspace concentration was measured by connecting tubes from the valves directly to a LICOR-820 gas analyzer which measured the headspace CO_2 concentration at about 60 mL min^{-1} flow rate.

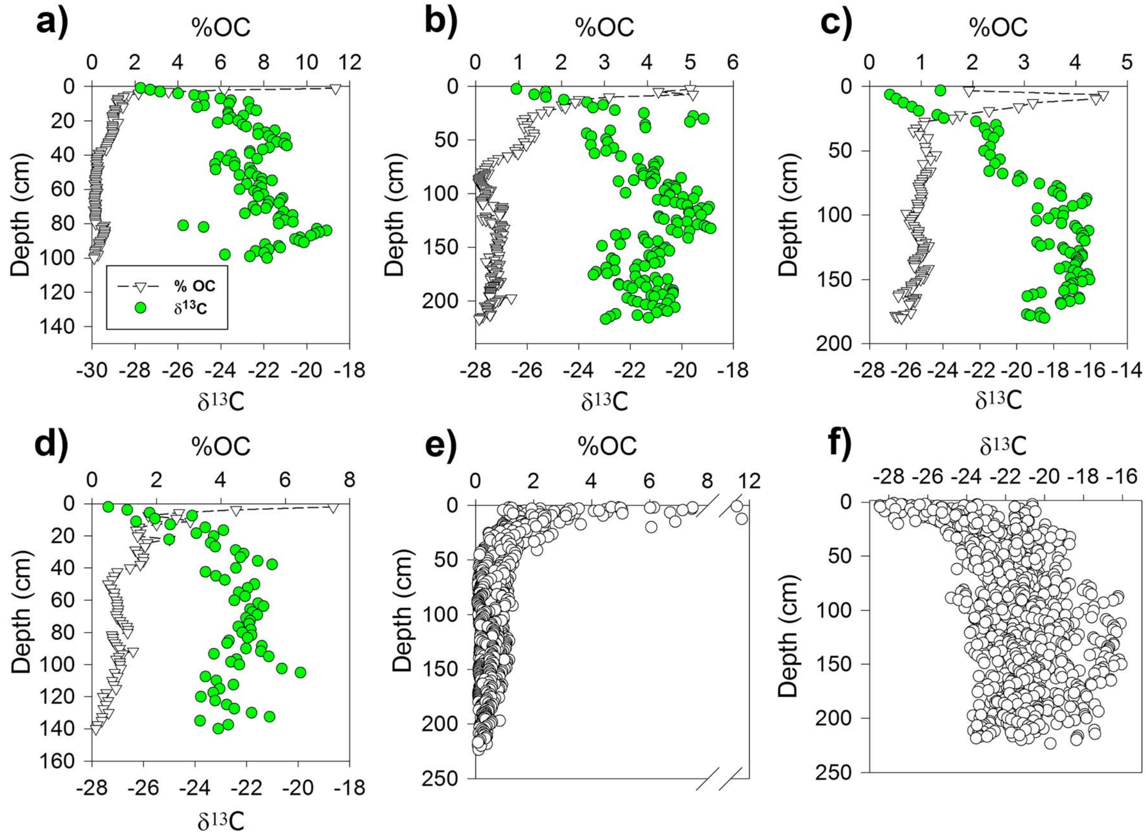

Figure 2. OC depth profiles for (a) Gadia, (b) Kiluluni, (c) LB Makere, and (d) Kajitupe. (e, f) The %OC and $\delta^{13}C$ depth profile for a combination of 30 sediment cores collected during this study.

The volume of the headspace in each jar was used to calculate the headspace concentration. After all the jars were sampled, they were opened, and water was added to compensate for any moisture loss. Subsequently, the jars were closed again, flushed with ambient air to remove the accumulated CO_2, and a new time zero sample was taken to represent the background concentration after which the samples were again stored in the incubation chamber for ~8 h.

3. Results

3.1. Depth-Integrated OC Patterns

Surface (<10 cm) OC contents under forested floodplain areas were significantly higher than under arable floodplain locations ($p < 0.01$, Mann-Whitney U test). Subsurface (10–50 cm) concentrations and those at greater depths (>50 cm) showed no relation between OC storage and current land use ($p = 0.24$, Mann-Whitney U test). Although profiles at different locations do show variations in OC, they all show a rapid reduction in OC to ~1% or below after an average of 60 cm depth (Figures 2a–2e). The $\delta^{13}C$ signature on the other hand shows a strong downcore tendency toward higher values from approximately −28 to −16‰ (Figure 2f) and depending on the prevailing land use (forested or arable land); the $\delta^{13}C$ signature was significantly different between landuse both in surface and subsurface depths ($p < 0.001$, Mann-Whitney U test), with the forested sites predominated with lighter signatures. The OC:TN ratio was on average low, with no particular trend with depth (supplementary information, S3) and there was a significant difference in OC:TN with land use for the surface layers ($p < 0.05$, Mann-Whitney U test) but not for the subsurface layers ($p = 0.22$, Mann-Whitney U test).

Floodplain sediments from all cores showed a dominance of fine grain sizes with >80% silt and clay in the upper 100 cm. Most sites had deeper layers similarly characterized by more than 70% silt and clay throughout the profiles down to depths where river bed sediment was encountered, which consisted of almost pure sand (Figure 3).

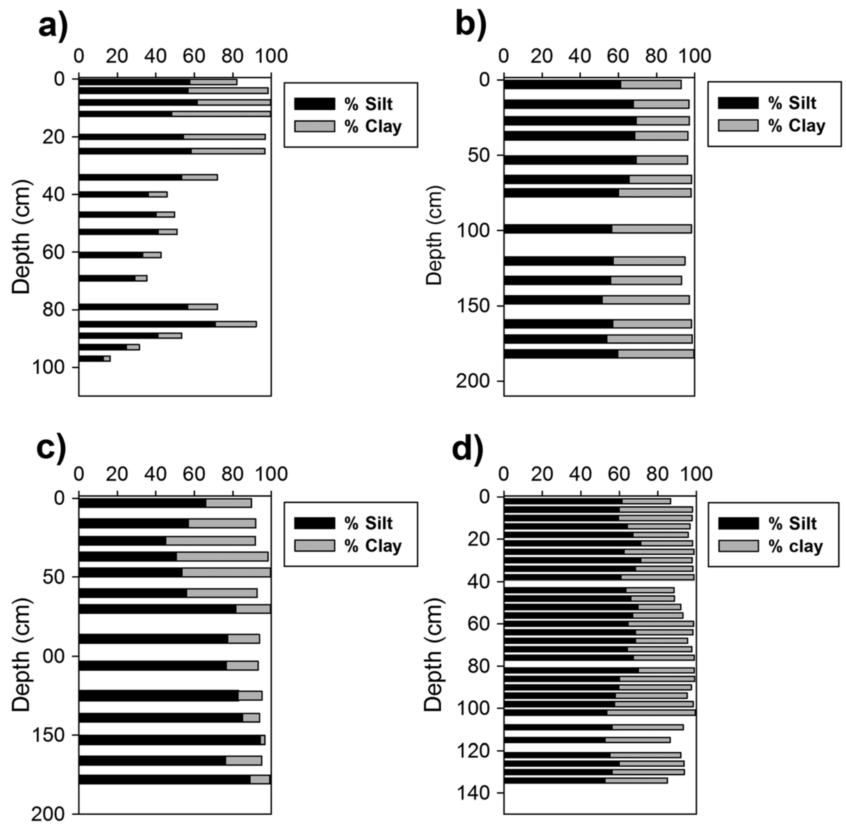

Figure 3. Examples of grain size distribution from four sites (a) Gadia, (b) Kiluluni, (c) LB Makere, and (d) Kajitupe. The dominance of clay and silt is evident throughout the majority of the profile.

3.2. Event Based POC Deposition Rates

The %OC in suspended river sediment (POC, Garissa-Garsen) and in fresh sediment deposits sampled after the 2013 flood event from the floodplain were relatively low and largely within the same range (Figure 4). The suspended sediments had an average of 1.58 ± 0.44% OC at Garissa and 1.32 ± 0.24% OC at Garsen, while within the floodplain a mean of 1.55 ± 0.40% OC was recorded in the freshly deposited materials. A statistical analysis showed that freshly deposited sediment %OC did not significantly differ from suspended sediment POC measurements observed at Garissa ($p = 0.66$, Wilcoxon test) but were significantly different from suspended sediment POC measurements at Garsen ($p < 0.05$, Wilcoxon test). The $\delta^{13}C_{OC}$ values of fresh sediment deposit samples averaged −22.4 ± 1.4‰ and did not differ significantly from the $\delta^{13}C_{POC}$ from either Garissa or Garsen ($p = 0.076$, Mann-Whitney U test) (Figure 4b).

3.3. Floodplain Respiration Rates

Different patterns in OC mineralization rates were observed when depth profile incubations were done under field or lab conditions (Figures 5a–5d and Figures 6a–6d). Under field conditions, OC mineralization rates increased with depth ($R^2 = 0.37$ and $p < 0.001$), whereas under lab conditions where moisture and temperature were standardized, a weak decrease was observed in mineralization rates with depth for most of the profiles ($R^2 = 0.16$ and $p < 0.01$). Moisture limitation seemed to greatly affect the incubations conducted under field conditions with an increase in respiration with increasing soil moisture content (Figure 7a). The % OC, on the other hand, had a strong influence on measured mineralization rates for lab incubations ($r_{spearman} = 0.56$, $p < 0.01$) (Figure 7b). The depth-integrated respiration rates over the top 1 m of the sediment profile were 1.22 mol C m^{-2} d^{-1} and 0.76 mol C m^{-2} d^{-1} for the lab and field incubations, respectively.

3.4. Radiocarbon Age

A single profile where a deep layer of overbank deposits was present and which was located in an actively flooding area was selected for ^{14}C analysis. At the surface, C age was near zero (i.e., nearly all C was modern).

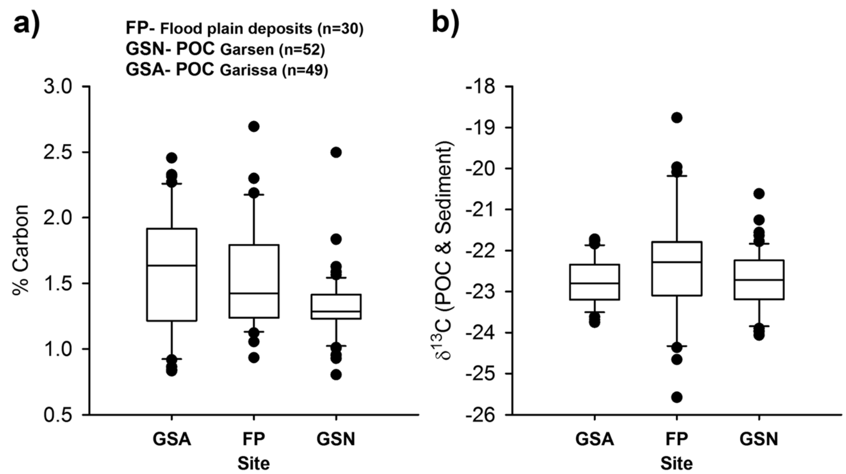

Figure 4. OC content of fresh sediment deposits from the floodplain (FP) and suspended sediment POC concentrations in Garissa (GSA) and Garsen (GSN) during the 2013 flood event. The center line, box extent, whiskers, and dots denote the 50th percentile, 25th and 75th percentiles, 10th and 90th percentiles, and outliers of estimates, respectively, for each site.

The subsurface C pool between 15 and 36 cm depth was relatively young (circa 600 B.P.) (Figure 8). Below this depth, OC age increased with depth, with ages of 1500–2700 B.P. toward the base of the core. In comparison, data from riverine suspended sediments also show on average close to modern signatures during the wet seasons (2008, 2010, and 2013) while more aged OC (up to 900 B.P.) was observed during the dry season (Figure 9).

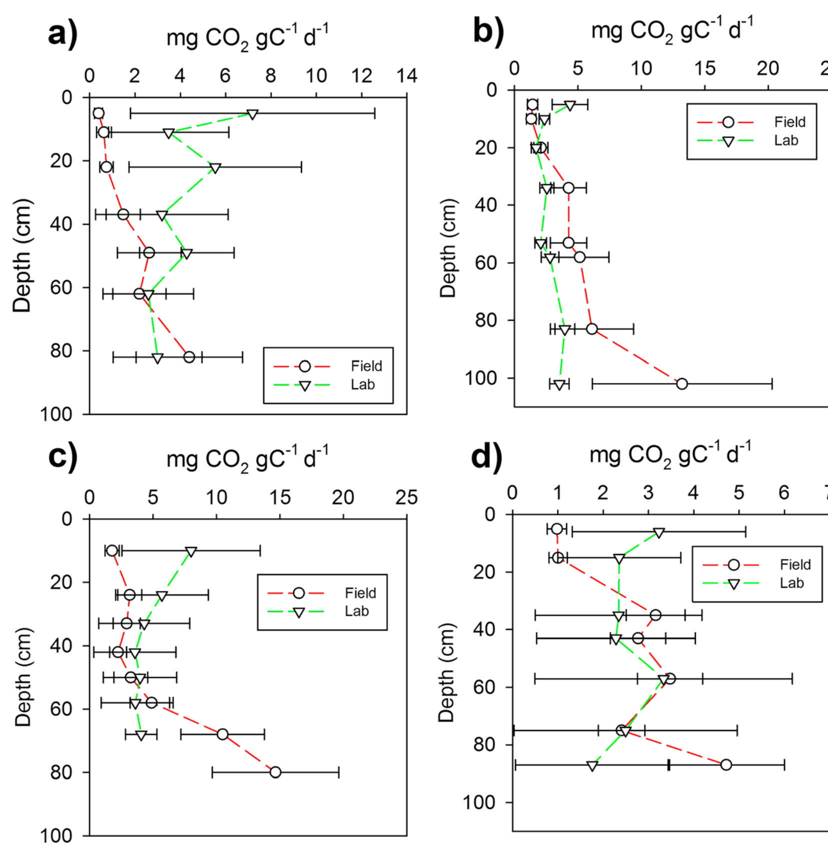

Figure 5. OM mineralization under field conditions (circles) and under lab conditions (triangles), for (a) Maroni I, (b) Mnazini, (c) Maroni II, and (d) Kipendi II. The error bars indicate the standard deviation over 7 days of measurements (field) and 16 days of measurements (lab).

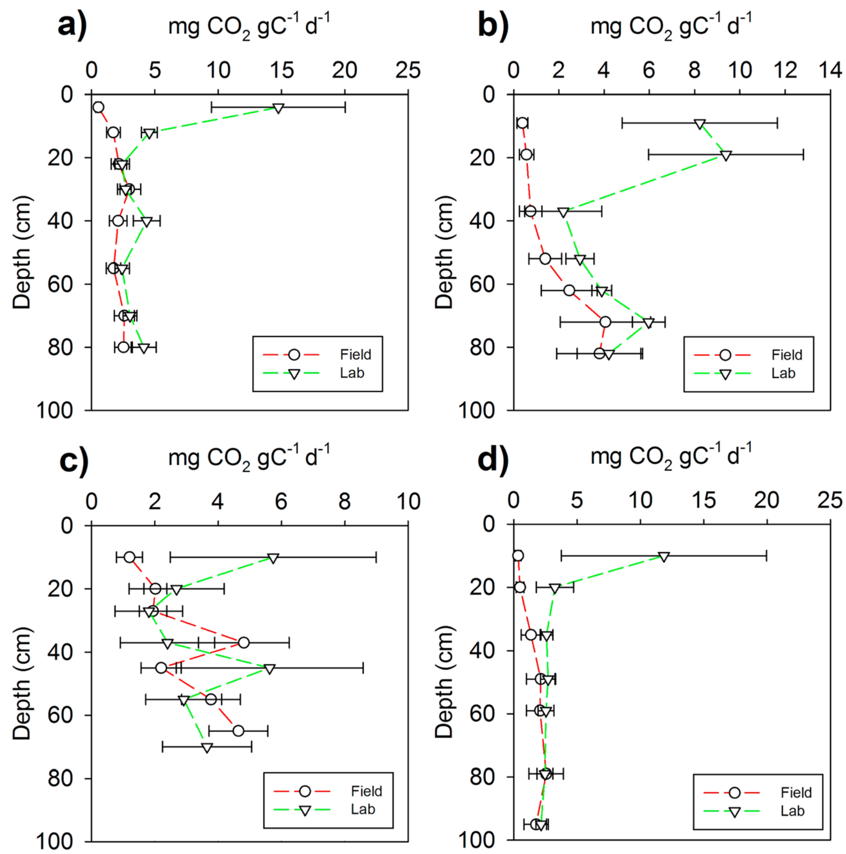

Figure 6. OM mineralization measured under field conditions (circles) and lab conditions (triangles), for (a) Wenje, (b) Kiembeni, (c) Ntunene I, and (d) Ntunene II. The error bars indicate the standard deviation over 7 days (field) and 16 days (lab) of measurements.

4. Discussion

4.1. Carbon Input Into the Floodplain

The Tana experiences semiannual flooding cycles that lead to deposition of sediments and OC within its adjacent floodplains. The fluvial sediments deposited contain between 1–3% OC by mass. Assuming a mean OC content of 1.56 ± 0.42% OC and floodplain sedimentation rates of 0.58–1.21 g cm^{-2} yr^{-1}, OC deposition rates

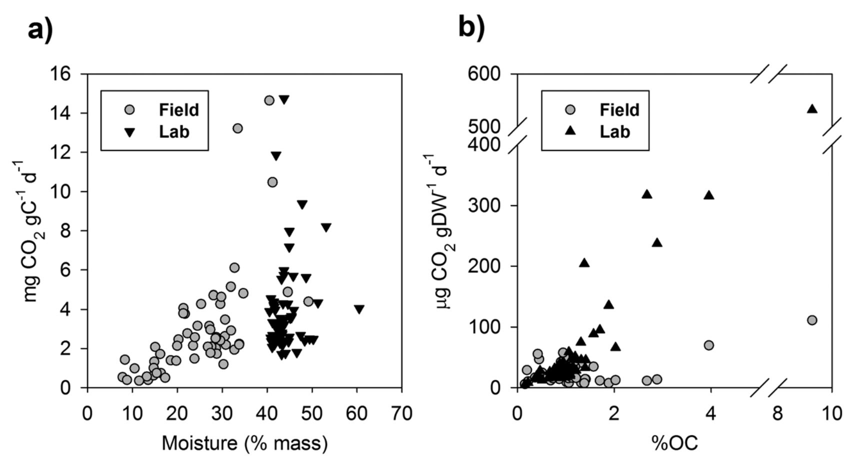

Figure 7. (a) Measured mineralization rates versus % moisture by mass in the sediments under field (circles) and lab (triangle) conditions and (b) measured mineralization rates (per unit total soil mass) versus OC. Field samples had variable moisture content, while the lab samples were all at ~60% WHC.

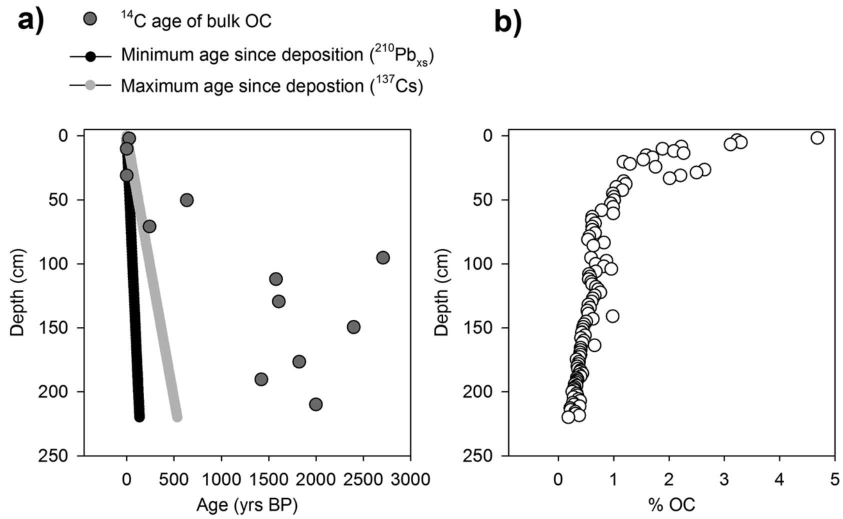

Figure 8. (a) ^{14}C dates (Kiluluni III) and (b) corresponding %OC profile for the same site. The profile shows that ^{14}C dates at depths below 30 cm are far older than the minimum and maximum sediment age. Sediment ages were estimated from a linear extrapolation of the sedimentation rates derived from fallout radionuclides $^{210}Pb_{xs}$ and ^{137}Cs. This potentially indicates post depositional selective mineralization of younger C and accumulation of aged riverine sediment.

are 0.91–1.89 t ha^{-1} yr^{-1} in the flooded areas. The Tana floodplain has a total surface area of ~998 km^2 but not all of this is subject to yearly flooding. Based on satellite imagery covering the Garissa-Garsen floodplain reach *Omengo et al.* [2016], as well as a historical discharge data at Garissa, the average annual flooded area is ~168 km^2. This implies that a total of 33 Gg OC yr^{-1} is deposited in the floodplain from overbank flow. This amount represents a substantial fraction of the annual POC flux at Garissa (estimated at 93–105 Gg OC yr^{-1}), [*Tamooh et al.*, 2014]. However, the amount of floodplain OC deposition is smaller than the total OC loss from the river system between Garissa and Tana Primate Reserve as estimated by *Tamooh et al.* [2014], (53–68 Gg C yr^{-1}), despite the fact that Tana Primate Reserve is located ~80 km upstream of Garsen.

A similar pattern was observed during the detailed monitoring campaign of the 2013 flood event, where a 61-day peak flow resulted in a flux of 4.61 Mt of suspended sediment and 73 Gg of OC at Garissa [*Geeraert et al.*, 2015b]. This peak flow resulted in a large flood, covering ~356 km^2 of the Tana floodplain and mean sedimentation rate was ~0.58 g cm^{-2}, resulting in the deposition of ~2.06 Mt of sediment and ~32 Gg of OC. Total losses of sediment and OC as derived from flux measurements at Garissa and Garsen were again larger, with a loss of 3.30 Mt of suspended sediment and of 56 Gg of OC.

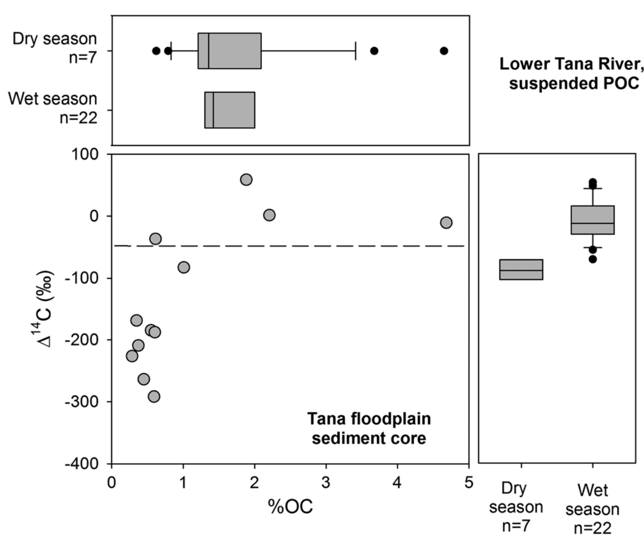

Figure 9. Δ^{14}C values and organic carbon content for Kiluluni III core in comparison to riverine sediment in the dry and wet seasons of 2008 and 2010 [*Bouillon et al.*, 2009; *Marwick et al.*, 2015] and 2013 (N. Geeraert et al., unpublished, 2015). The wet season signature is similar to that of OC found at the subsurface (<50 cm), above the dotted line.

These observations clearly demonstrate that processes other than floodplain deposition control the amount of OC lost from or gained by a river system. These processes include within-river POC mineralization, within-river POC deposition, mobilization of POC by lateral erosion of river banks and POC inputs from the terrestrial environment, e.g., by overland flow. Our data suggest that, for the lower Tana River, the losses of OC exceed the amount of OC deposition in the

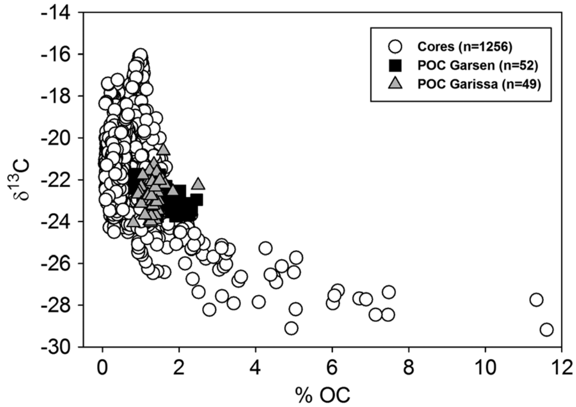

Figure 10. $\delta^{13}C$ values versus %OC for floodplain sediments (cores) and riverine POC at Garissa and Garsen. Floodplain sediments having a high %OC are clearly depleted in ^{13}C in comparison to riverine sediment because a significant fraction of the OC in these samples is derived from local biomass production. Floodplain sediments having a low OC content are enriched in ^{13}C in comparison to both riverine sediments and floodplain sediments having a high OC content, suggesting that their low OC content is related to selective mineralization.

floodplain, suggesting that other processes contributing to OC loss, such as within-river mineralization and deposition are also important.

Besides the deposition of sediment-derived POC, the production of terrestrial OC is important in the Tana River floodplain. The higher amount of % OC in the surface compared to riverine OC points to a postdepositional enrichment and a significant contribution to the OC pool from terrestrial biomass. This is confirmed by the low $\delta^{13}C$ signatures recorded in the upper layers of the flood deposits, which are generally between -28 and -26‰ (e.g., Figures 2a–2d and Figure 10), compared to values observed in riverine POC (-22.7 ± 0.7‰). The "new" light isotopic signature results from a contribution of floodplain vegetation utilizing the C_3 photosynthetic pathway. This terrestrial production significantly increases the total OC store that is present in the surface layers of the floodplain profile, with these top soils containing on average ~6% of OC.

4.2. Carbon Storage in the Floodplain

While it is clear that autochthonous OC production by floodplain vegetation significantly contributes to OC storage in the uppermost soil horizons, our data suggest that its contribution to deep OC burial is likely to be small. A first element to be considered is the $\delta^{13}C$ signature of the buried C. While the $\delta^{13}C$ signatures in the surface sediments clearly demonstrate the inputs from local C_3 vegetation, the $\delta^{13}C$ signatures increase strongly with depth to reach stable values at depths >60 cm (Figure 2f). An isotopic shift can be the result of kinetic fractionation during mineralization, resulting in an increased concentration of $\delta^{13}C$ by up to 4‰ in the residual OC if ~5% of the original C is preserved [*Wynn*, 2007]. As the $\delta^{13}C$ value of the topsoil material is -28‰ to -26‰, such fractionation could result in $\delta^{13}C$ of -24 to -22‰ in our case if 5% of the original OC is retained. However, the ^{13}C-enriched signatures found in deeper sediment layers are even heavier than -22‰ (up to -16‰), while the C content of the subsoil is often higher than 5% of that of the topsoil (e.g., Figure 2c). The fact that the $\delta^{13}C$ signature in the subsoil increases more strongly than what could be expected from kinetic fractionation alone can be better explained if the river derived OC, which has a higher $\delta^{13}C$ signature is considered as a separate, more recalcitrant pool, that is dominant in the subsoil. The observation that $\delta^{13}C$ signatures of the OC present in the subsoil are well higher than those of the riverine OC suggests that while the riverine OC persists longer than the autochthonous OC from floodplain vegetation, a significant fraction of the river OC is still relatively labile and may be further mineralized following burial. The latter is also suggested by the continuous marginal decline of total OC content with depth observed in most profiles. Furthermore, the ^{14}C dates show that the OC at depth is relatively old and significantly older than the age of sediment and OC deposition. A distinctly young age and inputs from vegetation can be seen in the top layers. When the $\Delta^{14}C$ ages at depth are compared with deposition ages derived from the deposition rates based on ^{137}Cs and $^{210}Pb_{xs}$, it is immediately clear that the minimum and maximum sedimentation ages are much smaller than the $\Delta^{14}C$ ages for all data points below ~50 cm (Figure 8). Therefore, the $\Delta^{14}C_{OC}$ data offer complementary evidence that only a recalcitrant fraction that is likely derived from riverine OC is preserved over longer time spans in the river deposits.

Finally, we noticed that soils under agricultural land have a different OC content in the top layers, but not in the subsoil. This again suggests that the amount of OC that is preserved over longer time spans does not depend on the amount of autochthonous OC input from floodplain vegetation. An uncertainty here is that no information is available about past land use in the area and that areas that are currently used for agriculture were under more natural vegetation in the past.

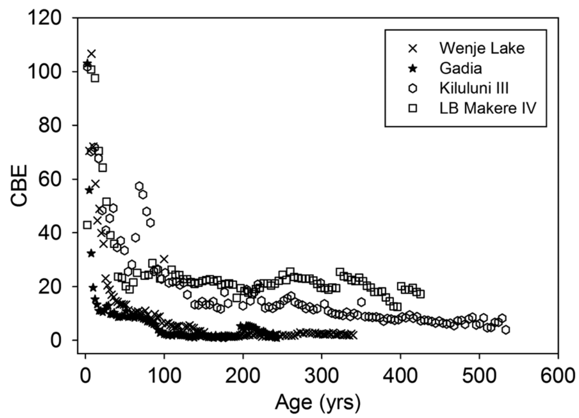

Figure 11. Variation of CBE with time for four sites. A relatively steep, indication rapid mineralization of surface OC is observed, the steepness decreases with time to a constant rate. However, over 70% of the initial OC is lost in less than a century.

All these patterns suggest that the C_3 inputs from local terrestrial vegetation do not contribute substantially to long-term OC burial. If this would be the case, one would not expect such a dramatic shift in ^{13}C signatures from the topsoil to the subsoil and one would expect the OC in the subsoil to be relatively recent. Furthermore, one may then expect that more OC would be stored in floodplains under forest, given that the C inputs to the topsoil are much higher in forested areas.

4.3. Floodplain OC Mineralization Rates

Our respiration experiments suggest that OC can be mineralized over the whole soil profile. This is confirmed by the observation that OC contents continue to decrease throughout the profile. The dry conditions leading to moisture limitation in the surface layers may explain why mineralization can still be relatively important at greater depths despite the fact that the OC at depth is more recalcitrant. The deeper parts of the soil profile will remain wet over much longer time spans thereby OC mineralization can continue over longer time spans. Given that Tana floodplains are in a warm climatic region, the frequent flooding and drying leads to seasonal fluctuations in water table depth. We expect mineralization and floodplain CO_2 production pulses to follow the same pattern and seasonality.

In the lab incubations, surface layers (<10 cm) recorded higher mineralization rates compared to the deeper sections of the profile ($p < 0.01$, Wilcoxon), suggesting that OC in top layers may be more labile than OC in deeper portions of the profile. Overall, the data indicate that a high percentage of the OC that is present in the surface layers is mineralized in a decadal time scale after burial. Indeed, the OC content of the floodplain sediments at depths below 60 cm is greatly reduced in comparison to the surface sediments. Based on the radionuclide inventories measured at the coring sites, such a depth corresponds to an age of circa 50–60 year [*Omengo et al.*, 2016]. The OC that remains in the soil at greater depths is more recalcitrant and rather slowly mineralized, leading to a more limited change in overall stocks below this depth.

Based on our data, we can calculate the overall carbon burial efficiency (CBE) by comparing how much of the surface OC is effectively buried assuming that the floodplain deposition rate is constant over time. The total OC in the surface layers shows an exponential decrease and a reduction down to 50% of the initial OC content in circa 50 years. Only a small fraction of the deposited OC, ranging between 5 and 20% of the surface OC, may be preserved for longer than a century. The variation of CBE over time confirms the hypothesis that the rate at which deposited OC is mineralized is initially high but decreases with time and that a more or less constant rate is reached after one century (Figure 11).

The CBE we observed is far lower than that observed by *Van Oost et al*. [2012] and *Wang et al*. [2014] in loamy soils in Belgium who found that it took several centuries (250–350 years) to mineralize half of the buried OC. One of the mechanisms to explain this difference is the average temperatures which are much higher in the Tana basin in comparison to Belgium and which may accelerate soil organic carbon (SOC) decomposition. On the other hand it should be noticed that the dry conditions occurring in the Tana basin during a large part of the year will reduce OC mineralization. The latter is likely to be more important than the temperature effect for the surface soils that are most prone to drying out between floods. Indeed, we observed relatively high SOC contents in the top layer of both forested and agricultural sites. Assuming mineralization rates similar to those under temperate, moist conditions, unrealistically high OC input rates would be necessary to maintain a topsoil SOC content of up to 6% in the surface layers and it may therefore be safely assumed that annual mineralization rates in the soil surface layer are relatively low. On the other hand it appears that large fraction of this topsoil SOC is mineralized relatively rapidly after burial. One factor which may explain this is that SOC contents of the topsoil are relatively high so that part of the OC is not well protected within soil aggregates [*Six et al*., 1998]. Another factor that may contribute in this case is the fact that moisture contents at greater depths are generally higher and conditions are more favorable for microbial activity, so that mineralization rates do not decline as fast with depth as they do under temperate conditions where the average soil moisture gradient within the soil profile will generally be smaller. Thus, both differences in environmental conditions and in the quality of the OC that is buried may explain why CBE is so low in the Tana floodplain.

Alternatively, we can take a riverine perspective and quantify the extent to which POC delivered by the Tana during flooding is stored over longer timescales, assuming as discussed earlier that floodplain vegetation inputs do not significantly contribute to long-term OC storage. If we assume that the OC in the subsoil is derived from riverine POC, and that riverine sediments contain on average, ~1.55% OC, burial efficiency is of course much higher (up to 80%) (supporting information Figure S5).

5. Conclusions

The Tana River floodplains trap substantial amounts of sediment and OC, thereby regulating their transport to the Indian Ocean. Deposited fluvial sediment is enriched in OC by local inputs from the floodplain vegetation. The burial of floodplain biomass is accelerated by subsequent flood events that deposit additional sediments which get mixed with the OC-enriched surface layer. However, a lot of the SOC that is buried is mineralized relatively quickly. Over 50% of available (sub) surface OC is decomposed in circa 30–50 years. Only a limited amount of OC (~10–20% of initial OC on the surface) is preserved over a much longer timescales.

Several of our observations, such as the δ^{13}C signature of the deeply buried OC as well as its ^{14}C age, suggest that most of the preserved OC consists of riverine OC. However, this riverine OC also undergoes further mineralization when buried in floodplain sediments over longer ($>$50 years) timespans.

The CBE in the tropical floodplain environment we studied here is much lower than the CBE observed in temperate, humid environments. This difference may be related both to differences in environmental conditions as well as to differences in the decomposability of the OC that is buried. A better quantification of CBE and an improved understanding of the factors controlling it is therefore clearly one of the ways forward toward a further refinement of global models that assess the effect of surface processes on the carbon cycle.

Acknowledgments
This work was supported by the Research Foundation Flanders (FWO-Vlaanderen, project G024012N), ERC-StG 240002 (AFRIVAL, http://ees.kuleuven.be/project/afrival/), and the KULeuven Special Research Fund (BOF). We especially thank Lore Fondu and Zita Kelemen for the assistance with laboratory work, the Kenya Wildlife Service (KWS) and Water Resources Management Authority (WRMA), Kenya for allowing access to different sites and availability of hydrological data, and the many field assistants who assisted in the coring and preparation of samples. Finally much appreciation for the two anonymous reviewers whose suggestions helped to substantially improve the manuscript. The full data used or cited in this paper can be requested from the authors (fredochieng.omengo@kuleuven.be, gerard.govers@kuleuven.be, or Steven.Bouillon@kuleuven.be)

References

Borges, A. V., et al. (2015), Globally significant greenhouse-gas emissions from African inland waters, *Nat. Geosci.*, doi:10.1038/ngeo2486.

Bouillon, S., et al. (2009), Distribution, origin and cycling of carbon in the Tana River (Kenya): A dry season basin-scale survey from headwaters to the delta, *Biogeosciences*, *6*, 2475–2493, doi:10.5194/bg-6-2475-2009.

Brown, T., and H. Schneider (1996), *Multi-Scale Estimates of Erosion and Sediment Yields in the Upper Tana Basin*, *Publ. Ser., 49–54*, IAHS, Kenya.

Cole, J. J., et al. (2007), Plumbing the Global Carbon Cycle: Integrating Inland Waters into the Terrestrial Carbon Budget, *Ecosystems*, *10*, 172–185, doi:10.1007/s10021-006-9013-8.

Dagg, M., T. Woodhead, and D. A. Rijks (1970), Evaporation in East Africa, *Int. Assoc. Scie. Hydrol. Bull.*, *15*, 61–67, doi:10.1080/02626667009493932.

Dearing, J. A., and R. T. Jones (2003), Coupling temporal and spatial dimensions of global sediment flux through lake and marine sediment records, *Global Planet. Change*, *39*, 147–168, doi:10.1016/S0921-8181(03)00022-5.

Dwars, Heederik en Verhey (1986), *Tana River Morphology Studies*, Delft Hydraulics Lab., Delft, Netherlands.

Galy, V., C. France-Lanord, O. Beyssac, P. Faure, H. Kudrass, and F. Palhol (2007), Efficient organic carbon burial in the Bengal fan sustained by the Himalayan erosional system, *Nature*, *450*, 407–410, doi:10.1038/nature06273.

Geeraert, N., P. M. Hermy, and P. S. Bouillon (2015a), *Hydrological Impacts on the Carbon Dynamics of Large Tropical River Systems Examination Committee*, KU, Leuven, Belgium.

Geeraert, N., F. O. Omengo, F. Tamooh, P. Paron, S. Bouillon, and G. Govers (2015b), Sediment yield of the lower Tana River, Kenya, is insensitive to dam construction: Sediment mobilization processes in a semi-arid tropical river system, *Earth Surf. Processes Landforms*, *40*, 1827–1838, doi:10.1002/esp.3763.

Gomez, B., L. A. K. Mertes, J. D. Phillips, F. J. Magilligan, and L. A. James (1995), Sediment characteristics of an extreme flood: 1993 upper Mississippi River valley, *Geology*, *23*, 963–966.

Hoffmann, T., S. Glatzel, and R. Dikau (2009), A carbon storage perspective on alluvial sediment storage in the Rhine catchment, *Geomorphology*, *108*, 127–137, doi:10.1016/j.geomorph.2007.11.015.

Hotchkiss, E. R., R. O. Hall, R. Sponseller, D. Butman, J. Klaminder, H. Laudon, M. Rosvall, and J. Karlsson (2015), Sources and control of CO2 emissions change with the size of streams and rivers, *Nat. Geosci.*, doi:10.1038/ngeo2507.

Hughes, F. M. R. (1988), The ecology of African floodplain forests in semi-arid and arid zones: A review, *J. Biogeogr.*, *15*, 127–140.

Hunsinger, G. B., S. Mitra, S. E. G. Findlay, and D. T. Fischer (2010), Wetland-driven shifts in suspended particulate organic matter composition of the Hudson River estuary, New York, *Limnol. Oceanogr.*, *55*, 1653–1667, doi:10.4319/lo.2010.55.4.1653.

Lal, R. (2003), Soil erosion and the global carbon budget, *Environ. Int.*, *29*, 437–50, doi:10.1016/S0160-4120(02)00192-7.

Maingi, J. K., and S. E. Marsh (2002), Quantifying hydrologic impacts following dam construction along the Tana River, Kenya, *J. Arid Environ.*, *50*, 53–79, doi:10.1006/jare.2000.0860.

Marwick, T. R., F. Tamooh, C. R. Teodoru, A. V. Borges, F. Darchambeau, and S. Bouillon (2015), The age of river-transported carbon: A global perspective, *Global Biogeochem. Cycles*, *29*, 122–137, doi:10.1002/2014GB004911.

Meade, R. H. (1996), River-sediment inputs to major deltas, in *Sea-level Rise and Coastal Subsidence*, pp. 63–85, Kluwer, London.

Medley, K. E. (1992), Patterns of forest diversity along the Tana River, Kenya, *J. Trop. Ecol.*, *8*, 353–371.

Omengo, F. O., T. Alleman, N. Geeraert, S. Bouillon, and G. Govers (2016), Sediment deposition patterns in a tropical floodplain, Tana River, Kenya, doi:10.1016/j.catena.2016.03.024, in press.

Rommens, T., G. Verstraeten, P. Bogman, I. Peeters, J. Poesen, G. Govers, A. V. Rompaey, and A. Lang (2006), Holocene alluvial sediment storage in a small river catchment in the loess area of central Belgium, *Geomorphology*, *77*, 187–201, doi:10.1016/j.geomorph.2006.01.028.

Schlünz, B., and R. R. Schneider (2000), Transport of terrestrial organic carbon to the oceans by rivers: Re-estimating flux- and burial rates, *Int. J. Earth Sci.*, *88*, 599–606, doi:10.1007/s005310050290.

Six, J., E. T. Elliott, K. Paustian, and J. W. Doran (1998), Aggregation and soil organic matter accumulation in cultivated and native grassland soils, *Soil Sci. Soc. Am. J.*, *62*, 1367, doi:10.2136/sssaj1998.03615995006200050032x.

Tamooh, F., F. J. R. Meysman, A. V. Borges, T. R. Marwick, K. Van Den Meersche, F. Dehairs, R. Merckx, and S. Bouillon (2014), Sediment and carbon fluxes along a longitudinal gradient in the lower Tana River (Kenya), *J. Geophys. Res. Biogeosci.*, *119*, 1340–1353, doi:10.1002/2013JG002358.

Van Oost, K., G. Verstraeten, S. Doetterl, B. Notebaert, F. Wiaux, N. Broothaerts, and J. Six (2012), Legacy of human-induced C erosion and burial on soil-atmosphere C exchange, *Proc. Natl. Acad. Sci. U.S.A.*, *109*, 19,492–19,497, doi:10.1073/pnas.1211162109.

Walling, D. E., P. N. Owens, and G. J. L. Leeks (1997), The characteristics of overbank deposits associated with a major flood event in the catchment of the River Ouse, Yorkshire, UK, *Catena*, *31*, 53–75, doi:10.1016/S0341-8162(97)00034-9.

Wang, Z., K. Van Oost, A. Lang, T. Quine, W. Clymans, R. Merckx, B. Notebaert, and G. Govers (2014), The fate of buried organic carbon in colluvial soils: A long-term perspective, *Biogeosciences*, *11*, 873–883, doi:10.5194/bg-11-873-2014.

Wang, Z., K. Van Oost, and G. Govers (2015), Predicting the long-term fate of buried organic carbon in colluvial soils, *Global Biogeochem. Cycles*, *29*, 65–79, doi:10.1002/2014GB004912.

Wynn, J. G. (2007), Carbon isotope fractionation during decomposition of organic matter in soils and paleosols: Implications for paleoecological interpretations of paleosols, *Palaeogeog. Palaeoclimatol. Palaeoecol.*, *251*, 437–448, doi:10.1016/j.palaeo.2007.04.009.